

Article

The Experimental Investigation of the Effects on the Combustion, Performance, and Emission Characteristics of an RCCI Engine Using Methanol/Diesel Fuel

Mustafa Temur^{1,2,*}, Cenk Sayin³ and Ilker Turgut Yilmaz³

¹ Department of Mechanical Engineering, Institute of Pure and Applied Sciences, Marmara University, 34854 Istanbul, Turkey

² Automotive Technology, Istanbul Gelisim University, 34310 Istanbul, Turkey

³ Faculty of Technology, Mechanical Engineering, Marmara University, 34854 Istanbul, Turkey; csayin@marmara.edu.tr (C.S.); ilker.yilmaz@marmara.edu.tr (I.T.Y.)

* Correspondence: mustafatemur@marun.edu.tr

Abstract: Reactivity-controlled compression ignition (RCCI) combustion is considered one of the most promising low-temperature combustion (LTC) concepts aimed at reducing greenhouse gases for the transportation and power generation sectors. RCCI combustion mode is achieved by combining different fuel types with low and high temperatures. The aim of this study is to investigate combustion characteristics and reduce nitrogen oxide (NO_x) and carbon dioxide (CO₂) emissions. In this experimental study, the effects of the RCCI strategy using methanol/diesel fuel on combustion characteristics (ignition delay, combustion duration), engine performance (brake-specific fuel consumption and brake-specific energy consumption), and emissions were examined in a four-cylinder, turbocharged, dual-fuel engine. The experiments were conducted at a constant speed of 1750 rpm at partial loads (40 Nm, 60 Nm, 80 Nm, and 100 Nm). The test results obtained with diesel fuel were compared with the test results obtained with methanol at different mass flow rates. When the results were examined, the minimum ignition delay (ID) occurred at 40 Nm torque, 5.63 crank angle (CA) with M12 fuel, while the maximum ID occurred with M26 fuel at 80 Nm torque, showing an increasing trend as engine load (EL) increased. The highest combustion time (CD) was achieved with M26 fuel at 100 Nm torque, whereas the lowest was achieved with the same fuel (M26) at 40 Nm. While the minimum brake-specific fuel consumption (bsfc) was 45.9 g/kWh for conventional diesel fuel at 40 Nm, the highest bsfc was 104.88 g/kWh for 100 Nm with M26 fuel. Generally, bsfc tends to increase with increasing load. Brake-specific energy consumption (bsec) had the lowest value of 1950.58 kJ/kWh with conventional diesel fuel at 40 Nm and the highest value of 4034.69 kJ/kWh with M26 fuel at 100 Nm. As the methanol content increased, significant improvements were observed in (NO_x) and (CO₂) emissions, while hydrocarbon (HC) and oxygen (O₂) emissions increased as well. Smoke emissions decreased at low loads but tended to increase at high loads.

Keywords: combustion; engine performance; emissions; methanol; RCCI engine



Citation: Temur, M.; Sayin, C.; Yilmaz, I.T. The Experimental Investigation of the Effects on the Combustion, Performance, and Emission Characteristics of an RCCI Engine Using Methanol/Diesel Fuel. *Energies* **2024**, *17*, 1436. <https://doi.org/10.3390/en17061436>

Academic Editors: Liwei Zhang and Haris Ishaq

Received: 8 February 2024

Revised: 10 March 2024

Accepted: 14 March 2024

Published: 16 March 2024



Copyright: © 2024 by the authors. Licensee MDPI, Basel, Switzerland. This article is an open access article distributed under the terms and conditions of the Creative Commons Attribution (CC BY) license (<https://creativecommons.org/licenses/by/4.0/>).

1. Introduction

Parallel to the rapidly increasing industrial developments worldwide, several challenges have emerged. The quest for alternative fuels to enhance the power capacity and fuel efficiency of internal combustion engines (ICE) in more environmentally friendly conditions has gained significant momentum. ICEs, a common engine type used in vehicles for many years, primarily rely on fossil fuels. However, the combustion of these fuels releases polluting gases into the environment through the exhaust, with known adverse effects on global warming, air pollution, and both the environment and human health. Compounding these issues is the fact that fossil fuel reserves are limited.

To address these challenges, scientists have directed their efforts toward researching alternative fuels suitable for internal combustion engines. For this purpose, alternative fuels are utilized either in their pure form or blended with petroleum-based fuels such as gasoline or diesel in internal combustion engines [1,2]. In order to leverage the distinctive properties of these alternative fuels, engine tests are conducted, involving adjustments to parameters like compression ratio (CR), ignition timing, and injection pressure.

Alcoholic fuels, including ethanol and methanol, are gaining attention as viable alternatives to gasoline in spark-ignition (SI) engines. The advantages presented by alcohol, derived from various sources and enhanced by cutting-edge technologies developed by industries, have spurred researchers to explore and capitalize on their potential benefits [3].

Methanol is the most promising and researched fuel among the fuels considered as an alternative to gasoline. Pure methanol and different percentages of methanol–gasoline mixtures have been extensively tested on engines in recent years. On the other hand, research on utilizing methanol as a vehicle fuel began in the 1980s. In China, they developed fuel kits to utilize both M85 (comprising 85% methanol and 15% gasoline) and M100 (pure methanol) fuels. There are also disadvantages to using gasoline–alcohol mixtures as fuel. One of these problems is alcohol’s tendency to react with water. When this occurs, the alcohol separates locally from the gasoline, creating an inhomogeneous mixture. This causes the engine to run erratically due to large fuel–air ratio differences between the two fuels. Automobile companies conduct tests on engines that can use any gasoline–methanol–ethanol composition. As a result, methanol is predominantly produced for chemical purposes rather than as a dedicated fuel source. Presently, methanol plays a crucial role in the production of waste frying oil methyl ester (biodiesel), a mandatory component in many countries [4,5].

Methanol fuel is used in some dual-fuel diesel engines. Methanol is not a good diesel engine fuel alone. However, good results are achieved in diesel engines with methanol if a small amount of diesel fuel is used to achieve ignition. Methanol is an attractive fuel in some countries where it is much cheaper to produce than diesel fuel. In the experiments carried out on methanol, old diesel bus engines were converted to run on methanol. As a result of these experiments, improvements were observed in all harmful emissions compared to the old type of diesel engine running on diesel fuel. Methanol as a fuel presents several advantageous opportunities. Some of these include the production of methanol from renewable resources, as well as readily available high-ash coal, municipal solid waste, and low-value biomass. Methanol-powered engines produce lower emissions compared with baseline mineral diesel-fueled engines, exhibit less combustion noise than equivalent diesel engines, and offer higher land use efficiency than other cultivable renewable fuels [6].

Physical and Chemical Properties of Methanol

In this part, general information is given about the physical and chemical properties of methanol, which is used as a renewable alternative fuel in ICs. Methanol is a type of alcohol that is colorless, has a barely perceptible odor, and is significantly toxic. It can especially affect the nervous system and cause blindness. Even though it is unlikely, taking it orally can have fatal consequences. Its vapor can penetrate a person through the lungs, and methanol liquid can penetrate the skin. Gasoline and diesel are not equally dangerous. The reason is that their taste and smell make them noticeable much more quickly than methanol. Gasoline and diesel fuels should also be used with caution, but they are not as dangerous as methanol [7].

Methanol is an alcohol fuel, such as ethanol, butanol, and propanol. The most important advantage of alcohol fuels is their low viscosity compared with diesel fuel. Therefore, it can be easily injected, atomized, and mixed with air. In addition, the high laminar combustion rate, which can ensure that the combustion process ends earlier, increases the thermal efficiency of the engine. Less emissions occur due to high oxygen content and low sulfur content [8]. Some chemical and physical properties of methanol and diesel fuels are shown in Table 1 [9–11].

Table 1. Some physical and chemical properties of diesel and methanol.

Fuel Specifications	Diesel	Methanol
Chemical formula	C ₁₂ H ₂₄	CH ₃ OH
Density (kg/m ³ 293 °K)	847	795
Ignition temperature (°K)	483–523	743
Lower calorific value (MJ/kg)	42.5	20.1
Latent heat of vaporization (kJ/kg)	260	1100
Cetane number	51	<5
Octane number	17	111
Latent burning speed (cm/s)	-	523
Stoichiometric air/fuel ratio	14.3	6.5
Viscosity (mm ² /s 313 K)	2.72	0.58
Boiling point (°C)	180–360	64.5

Many recent studies focus on low-temperature combustion (LTC) strategies that can reduce emissions and improve fuel economy. Three common strategies for achieving LTC are known as homogeneous charge compression ignition (HCCI), premixed charge compression ignition (PCCI), and reactivity-controlled compression ignition (RCCI).

Recent experimental and simulation results show that RCCI is a more promising technology than the other two strategies, HCCI and PCCI. This method is important in terms of providing more effective ignition control and having a low maximum ROPR. Additionally, RCCI has been observed to maintain low emissions and high fuel efficiency simultaneously [12]. RCCI, defined as a combustion technology in dual-fuel engines, involves the utilization of at least two fuels with differing reactivity levels for in-cylinder fuel blending. This method employs a multiple injection strategy and an optimal EGR (exhaust gas recirculation) rate to regulate in-cylinder reactivity. The ultimate goal is to enhance combustion phasing, duration, and magnitude, consequently resulting in improved brake thermal efficiency (BTE) while minimizing both NO_x and smoke emissions [13,14]. The RCCI combustion system demonstrates its versatility by operating effectively over a wide range of engine loads from 4.6–14.6 bar gross IMEP. This operational range achieves nearly negligible levels of NO_x and smoke emissions, ensuring compliance with regulatory standards. Additionally, it maintains acceptable ROPR and minimal ringing intensity while delivering remarkably high indicated efficiency [15,16].

There are many publications in the literature on the use of methanol and alcohol fuels in ICes. However, the methods and results of some publications on the use of methanol and alcohol fuel in RCCI combustion strategies are summarized below:

In their experimental study, Panda and Ramesh conducted research to obtain low emissions and high BTE of the RCCI engine using methanol/diesel fuel. Tests were carried out on a single-cylinder, common-rail water-cooled diesel at a constant speed of 1500 rpm and an average indicated effective pressure of 5 bar. Energy sharing from methanol to diesel can be increased from 45% in dual-fuel mode to nearly 56% in RCCI mode by appropriately adjusting the injection parameters. In this case, while the BTE increased from 36% to 38%, NO_x emission was found to be 95% lower in RCCI mode. Smoke emissions have been reduced by 78%. In order to increase the BTE to 42%, more than 45% ES from methanol to diesel is required after heating the intake air to approximately 85 °C. In this case, it was observed that while NO_x emissions decreased, carbon monoxide (CO) and HC emissions increased [17].

Agarwal et al. used fuels with different methanol premixed ratios (M30, M50, M80) in a two-cylinder, common-rail direct-injection and turbocharged RCCI engine and compared them with diesel fuel. Bsec decreased between M30 and M80. HC and CO increased in more methanol fractions. CO₂ and smoke emissions decreased compared with conventional diesel fuel. While NO_x emissions decreased in M30 and M50 fuels, they increased in M80 fuels [18].

Duraisamy et al. examined the effects of methanol/diesel and methanol/PODE dual-fuel RCCI combustion in a three-cylinder, common-rail direct injection, turbocharged diesel engine. The tests were carried out at 3.4 bar brake mean effective pressure (BMEP) and 1500 rpm engine speed. When the results were examined, the researchers observed that the ID lengthened as the mass of methanol increased in both methanol/diesel and methanol/PODE processes. With the increase of methanol mass fraction, NO_x and smoke emissions for RCCI combustion decreased significantly. However, it was determined that HC and CO emissions increased slightly [19].

Hassan et al. conducted a study using methanol and diesel fuels in a single-cylinder, 2000 rpm constant engine speed, air-cooled engine. In the experimental procedure, pure diesel and methanol content by mass of 7%, 14%, and 21% (MD7, MD14, and MD21) were used as fuel. In the experimental results, it was observed that bsec and bsfc decreased in MD7 and MD14 but increased in MD21 fuel compared with pure diesel fuel [20].

In their study, Huang et al. conducted research on a four-cylinder, turbocharged, direct-injection RCCI engine at a constant speed of 1800 rpm. They examined the effects of EGR and different methanol substitution rates on combustion, performance, and emissions of methanol/diesel fuels. HC and CO emissions increased with the increase of bsfc at 90% load. As the methanol substitution rate increased from 0% to 30%, bsfc decreased by 3.29%. Increased HC and CO emissions were observed with the use of EGR. Significant improvements were observed in NO_x emissions by 73.6%, with a 30% increase in the methanol substitution rate [21].

In their study, Liu et al. conducted an experimental study on a turbocharged, inter-cooled four-cylinder RCCI engine using diesel/methanol dual fuel at a low load. In the study conducted at 1800 rpm and 30% load, HC emissions decreased when the methanol content increased from 40% to 60% at low loads. It was observed that NO_x and smoke emissions increased [22].

When the literature studies are examined, it is noted that the effects of ID, CD, engine performance parameters such as bsfc, bsec, and exhaust emissions have not been investigated in the methanol/diesel dual-fuel RCCI engine, at a constant engine speed (1750 rpm), in four different ELs (40, 60, 80, and 100 Nm), and with different methanol energy fractions (M12, M19, and M26).

2. Materials and Methods

A four-cylinder, water-cooled, turbocharged, common-rail diesel engine was used in the experiments. The schematic diagram of the experimental setup is shown in Figure 1 and the specifications of the experimental engine are shown in Table 2.

Table 2. Features of the experimental engine.

Engine Specifications	
Type	In-line, turbocharged
Number of cylinders	4
Bore	76 mm
Stroke	80.5 mm
Number of valves	8
Cylinder volume	1461 cm ³
Compression ratio	18.25:1
Maximum power (4000 rpm)	48 kW (65 hp)
Maximum torque (1750 rpm)	160 Nm
Fuel injection	Common-rail
Type	In-line, turbocharged

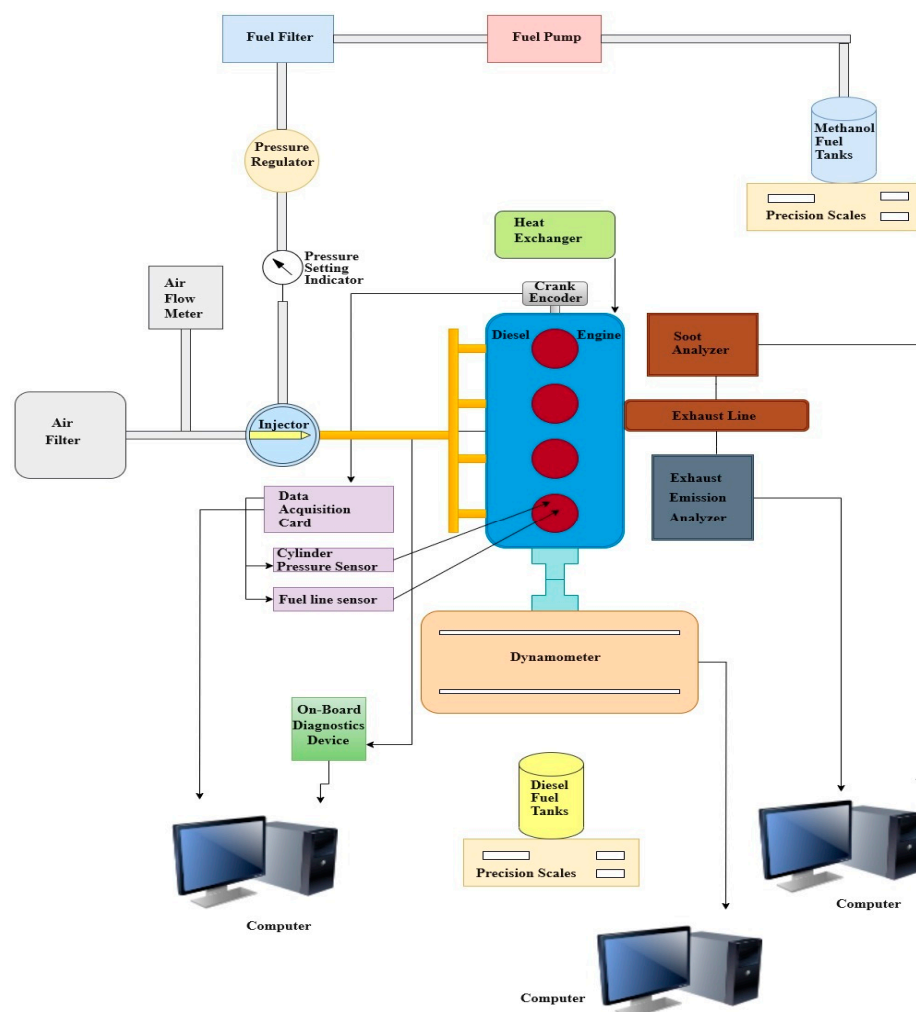


Figure 1. Schematic diagram of experimental setup.

The experimental engine was loaded with an Eddy Current dynamometer (Cussons P8602) with maximum torque, maximum power, and a maximum speed of 475 Nm, 160 kW and 8000 rpm, respectively. Dynamometer software called MOTEST 6.3.126 was used in the experiments. Thanks to this software, many parameters such as engine power, torque and speed, oil temperature, fuel temperature, cooling water inlet and outlet temperatures, intake air and exhaust gas temperature are read and recorded.

The diesel motor was outfitted with a cylinder pressure sensor, a fuel line pressure sensor, and a crank encoder. A piezoresistive pressure transducer (Kistler, 4067 C2000AO) paired with a charge amplifier was affixed to the fuel line of the first cylinder's injector. The position of the crankshaft was determined using the crank encoder with a 0.35 CA resolution, and a data acquisition card (National Instruments, 6343) was employed to collect and store data on cylinder gas and injection line pressure for the analysis of combustion. The data obtained from the cylinder pressure and fuel line sensor installed on the first cylinder shown in Figure 1 can be seen in the combustion analysis program. The signals transmitted from the amplifier are transferred to a computer via the National Instrument data acquisition card, and cylinder pressure and fuel line pressure data are recorded simultaneously.

The diesel fuel to be used in the experiments was obtained from TUPRAS (Turkish Petroleum Refineries Corporation). Methanol, with a purity of 99%, was purchased from a commercial supplier.

In this study, exhaust emission measurements were conducted using a Bosch BEA 460 model emission device. Exhaust gases (HC, CO₂, O₂, NO_x, and smoke) drawn into

the emission device through a pipe connected to the engine's exhaust line were measured and recorded. Exhaust emission measurement points were determined by drilling two holes in the exhaust line pipe and connecting smoke and emission analyzers to these points. A Bosch brand soot emission analyzer was used for heat measurement. The data from the emission devices are read from the computer using Bosch BEA 460 emission analysis software. The characteristics of the emission device are given in Table 3.

Table 3. Emission device features.

Features	Measuring Range	Sensibility
Hydrocarbon (HC)	0–10,000 ppm	1 ppm
Oxygen (O ₂)	0–22% vol.	0.01% vol
Nitrogen oxide (NO _x)	0–5000 ppm	1 ppm
Carbon dioxide (CO ₂)	0–18% vol.	0.01% vol
Air excess coefficient	0.5–1.8	0.001
Absorption coefficient (K)	0–10 m ⁻¹	0.01 m ⁻¹

Methanol fuel was sent from a tank through the fuel pump, fuel filter, and pressure regulator to the intake manifold. There was a pressure change indicator on the intake manifold. Both methanol and diesel fuel consumption were measured with a precision scale. The amount of fuel consumed per minute was measured with a stopwatch. Experiments were carried out under different ELs (40, 60, 80, and 100 Nm) at a constant speed of 1750 rpm. The experiments were conducted under partial load conditions. At maximum torque (1750 1/min), 25% of the full load (160 Nm) corresponded to 40 Nm, 37.5% to 60 Nm, 50% to 80 Nm, and 62.5% to 100 Nm. The experiments were performed at these torque values. The experimental engine was heated to 85–90 °C and stabilized to reach the desired experimental conditions. The experiments were repeated three times, and data were collected by stabilizing the engine before each experiment.

Measurement sensitivities and calculated uncertainties are presented in Table 4. The Kline and McClintock method [23,24] was applied to determine the measurement sensitivities and total uncertainty analysis values of the equipment. The methanol energy fraction is calculated using the following Equation (1):

$$MEF = LHV_{CH_3OH} \cdot \dot{m}_{CH_3OH} / LHV_D \cdot \dot{m}_D + LHV_{CH_3OH} \cdot \dot{m}_{CH_3OH} \quad (1)$$

MEF is methanol energy fraction. Figure 2 shows the energy-sharing rates of diesel/methanol fuels used in the experiments as a percentage. It shows how much energy is provided by which type of fuel.

Table 4. Measurement sensitivities and calculated uncertainties.

Parameter	Device	Accuracy
Engine torque	Load cell	±0.25%
Engine speed	Crank encoder	±0.1%
Cylinder pressure	Oprand 32288GPA	±0.5%
Fuel pressure	Kistler, 4067	±0.05%

\dot{m}_D and \dot{m}_{CH_3OH} are the mass flow rates of methanol and diesel fuel in kg/h, and LHV_{CH_3OH} and LHV_D are lower heating values of methanol and diesel fuel in MJ/kg.

The energy requirement of the engine increased as the EL values increased. This study was carried out by increasing the amount of diesel fuel to meet the increased energy demand. The methanol rates at the M12, M19, and M26 levels were fixed for their values at all ELs in this study.

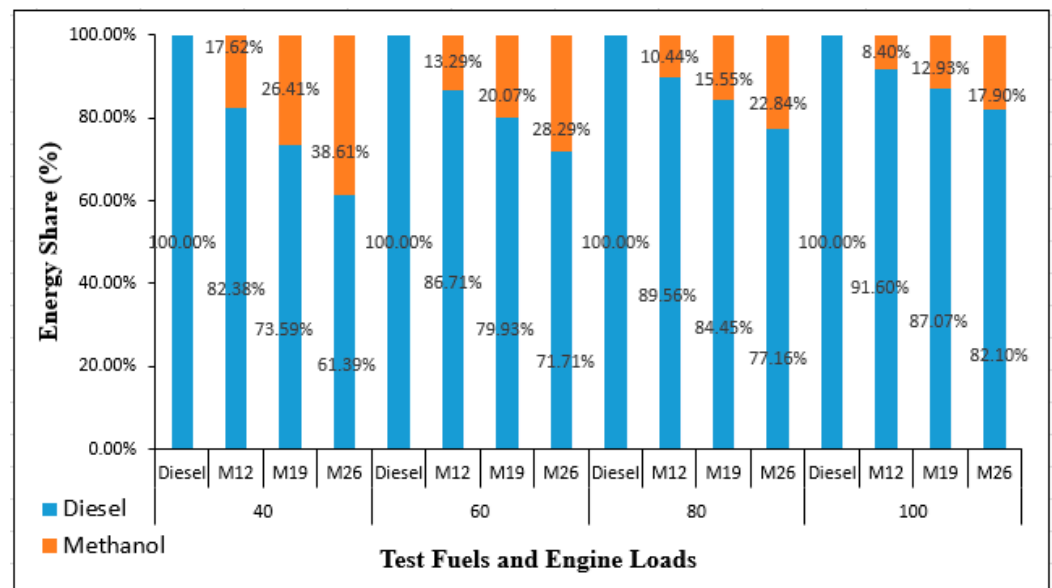


Figure 2. The energy shares of test fuels in percentage.

Data Analysis

Calculation of Brake-Specific Fuel Consumption

Diesel and methanol fuels were measured with precision scales. The amounts of diesel fuel injected from the main injection and the fuel injected from the port injection were measured in one minute, and the *bsfc* was calculated.

$$\dot{m} = \frac{V_y \cdot \rho_y \cdot 10^{-3} \cdot 3600}{t} \quad (2)$$

In the formula here,

\dot{m} = fuel mass flow rate (kg/h),

V_y = fuel volume (L),

ρ_y = fuel density (kg/m³), and

t = time (s) was used.

In order to calculate *bsfc*, the fuel mass flow rate in Equation (2) is written into Equation (3) [25].

$$bsfc = \frac{\dot{m}}{N_e} \cdot 10^3 \quad (3)$$

N_e is the engine power in the equation.

Calculation of Brake-Specific Energy Consumption

bsec is a parameter expressed as the power or work obtained from the test engine in terms of the unit of fuel or energy consumed. It is found by multiplying the *bsfc* by the lower heating values (LHV) of the fuels [26].

$$bsec = bsfc \cdot LHV \quad (4)$$

bsec: specific energy consumption (kJ/kWh).

bsfc: specific fuel consumption (kg/kWh).

LHV: lower calorific value of the fuel (kJ/kg).

3. Results

A comparative evaluation of IDs and CDs was made in different ELs for both standard diesel engines and RCCI combustion modes. Combustion parameters are given in the table below Table 5.

Table 5. Combustion characteristics of the fuels for different engine conditions.

EL	Parameter	Unit	Diesel	M12	M19	M26
40 Nm	SOI	$^{\circ}\text{CA}$	339.26	339.26	345.94	348.05
		$\text{J}/^{\circ}\text{CA}$	0.87	0.27	0.24	0.35
	Maximum CP	$^{\circ}\text{CA}$	364.57	365.63	366.33	368.44
		$\text{MPa}/^{\circ}\text{CA}$	83.48	86.56	87.24	89.55
	ID	$^{\circ}\text{CA}$	5.98	5.63	11.25	10.20
	CD	$^{\circ}\text{CA}$	62.58	62.23	55.55	53.09
60 Nm	SOI	$^{\circ}\text{CA}$	342.07	342.42	344.53	345.59
		$\text{J}/^{\circ}\text{CA}$	0.01	0.27	0.36	0.38
	Maximum CP	$^{\circ}\text{CA}$	364.92	365.27	365.98	366.33
		$\text{MPa}/^{\circ}\text{CA}$	88.97	93.45	95.03	99.29
	ID	$^{\circ}\text{CA}$	13.01	13.01	13.36	11.60
	CD	$^{\circ}\text{CA}$	61.52	61.17	58.71	57.30
80 Nm	SOI	$^{\circ}\text{CA}$	340.66	341.02	342.07	343.83
		$\text{J}/^{\circ}\text{CA}$	0.30	0.55	0.36	0.62
	Maximum CP	$^{\circ}\text{CA}$	377.58	366.68	365.98	365.63
		$\text{MPa}/^{\circ}\text{CA}$	105.57	103.27	105.33	109.56
	ID	$^{\circ}\text{CA}$	12.66	14.41	15.12	15.12
	CD	$^{\circ}\text{CA}$	61.17	62.58	62.93	61.52
100 Nm	SOI	$^{\circ}\text{CA}$	338.91	339.26	340.31	340.66
		$\text{J}/^{\circ}\text{CA}$	0.38	0.27	0.11	0.33
	Maximum CP	$^{\circ}\text{CA}$	377.23	375.82	375.47	371.25
		$\text{MPa}/^{\circ}\text{CA}$	117.97	114.86	116.31	117.89
	ID	$^{\circ}\text{CA}$	12.30	14.77	13.71	13.36
	CD	$^{\circ}\text{CA}$	62.23	62.58	63.98	64.34

Shown in Table 5, SOI is start of ignition, Maximum CP is maximum cylinder pressure, ID is ignition delay, and CD is combustion duration. Fuel types M12, M19, and M26 show mass flow rates at different pressures.

3.1. Combustion Characteristics

3.1.1. Ignition Delay

ID is defined as the time between the injection of fuel into the combustion chamber and the moment when the first flame nucleus forms in the combustion chamber. In this study, the start of injection was determined as the $^{\circ}\text{CA}$ corresponding to the first sudden drop in fuel line pressure. The fuel line pressure opened at 330 CAs. The beginning of combustion was identified as the $^{\circ}\text{CA}$ at which the pressure increase rate was maximum. The time interval between these two states is defined as the ID in CA.

As shown in Figure 3, the ID is set as 5.98 $^{\circ}\text{CA}$ for diesel fuel, 5.63 $^{\circ}\text{CA}$ for M12 fuel, 11.25 $^{\circ}\text{CA}$ for M19 fuel, and 10.20 $^{\circ}\text{CA}$ for M26 fuel at a 40 Nm load. The maximum ID increase rate obtained by using diesel fuel at a 40 Nm load decreased by 5.85% with M12 fuel, 88.13% with M19 fuel, and 70.57% with the use of M26 fuel.

ID is set as 13.01 $^{\circ}\text{CA}$ for diesel fuel, 13.01 $^{\circ}\text{CA}$ for M12 fuel, 10.55 $^{\circ}\text{CA}$ for M19 fuel, and 11.60 $^{\circ}\text{CA}$ for M26 fuel at a 60 Nm load. The maximum ID increase rate obtained by using diesel fuel at a 60 Nm load was constant at the same rate as with M12 fuel, then decreased by 18.91% with M19 fuel and 10.84% with the use of M26 fuel.

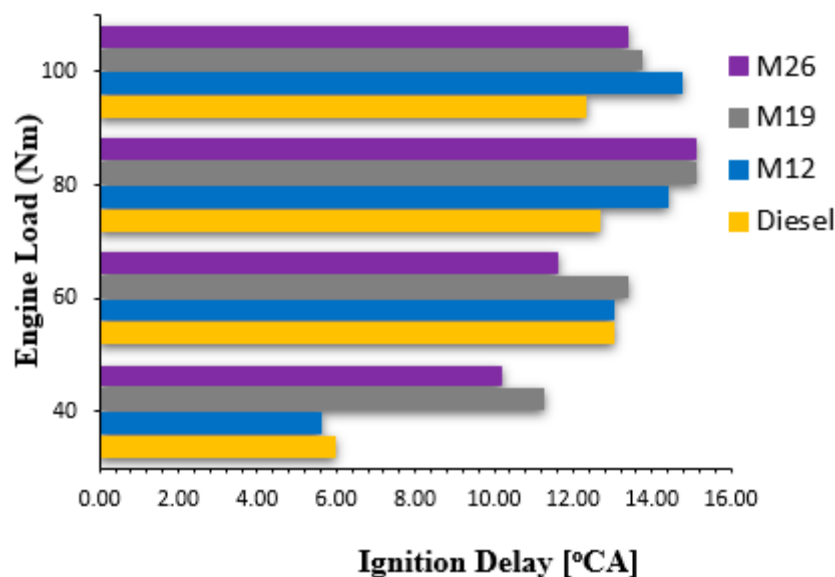


Figure 3. IDs in terms of °CA for different fuels at 40 Nm, 60 Nm, 80 Nm, and 100 Nm ELs.

ID is set as 12.66 °CA for diesel fuel, 14.41 °CA for M12 fuel, 15.12 °CA for M19 fuel, and 15.12 °CA for M26 fuel at an 80 Nm load. The maximum ID increase rate obtained by using diesel fuel at an 80 Nm load is 13.82% with M12 fuel, 19.43% with M19 fuel, and 19.43% with the use of M26 fuel.

ID is set as 12.30 °CA for diesel fuel, 14.77 °CA for M12 fuel, 13.71 °CA for M19 fuel, and 13.36 °CA for M26 fuel at a 100 Nm load. The maximum ID increase rate obtained by using diesel fuel at a 100 Nm load is 20.08% with M12 fuel, 11.46% with M19 fuel, and 8.62% with the use of M26 fuel.

In RCCI mode, as the methanol content increased, the ID increased. The highest increase was 88.13%, with M19 fuel at 40 Nm. As the load increases, the ID increases. If the ID increases, combustion starts later. Long-term ID sometimes leads to a better air–fuel mixture, which affects heat release. It is known that alcohol fuels generally increase the ID compared with diesel fuel due to their lower cetane numbers [27]. It is seen that the ignition delay decreases at the high load of 100 Nm due to the effect of increasing load and the decrease in the percentage of methanol in M26 fuel. This is thought to be due to the decrease in the energy fraction of methanol, which is a high octane number fuel. In addition, due to the higher latent heat of condensation of methanol, the in-cylinder temperature may increase with the decreasing energy fraction, which may reduce the ignition delay as seen in 100 Nm and M26 fuel [19].

3.1.2. Combustion Duration

The CD is a critical parameter that should be considered in alcohol fuels. The alteration in combustion time, compared with conventional fuels, significantly influences the performance and emission results of ICE. The CD was calculated as the difference between the CA at the CHR and the start of combustion.

As seen in Figure 4, CDs are shown for different loads. The CD at a 40 Nm load was found to be 62.58 °CA for diesel fuel, 62.23 °CA for M12 fuel, 55.55 °CA for M19 fuel, and 53.09 °CA for M26 fuel. The CD obtained by using diesel fuel at a 40 Nm load decreased by 0.56% with M12 fuel, 11.23% with M19 fuel, and 15.16% with M26 fuel.

The CD at a 60 Nm load is found to be 61.52 °CA for diesel fuel, 61.17 °CA for M12 fuel, 58.71 °CA for M19 fuel, and 57.30 °CA for M26 fuel. The CD obtained by using diesel fuel at a 60 Nm load decreased by 0.57% with M12 fuel, 4.57% with M19 fuel, and 6.86% with the use of M26 fuel.

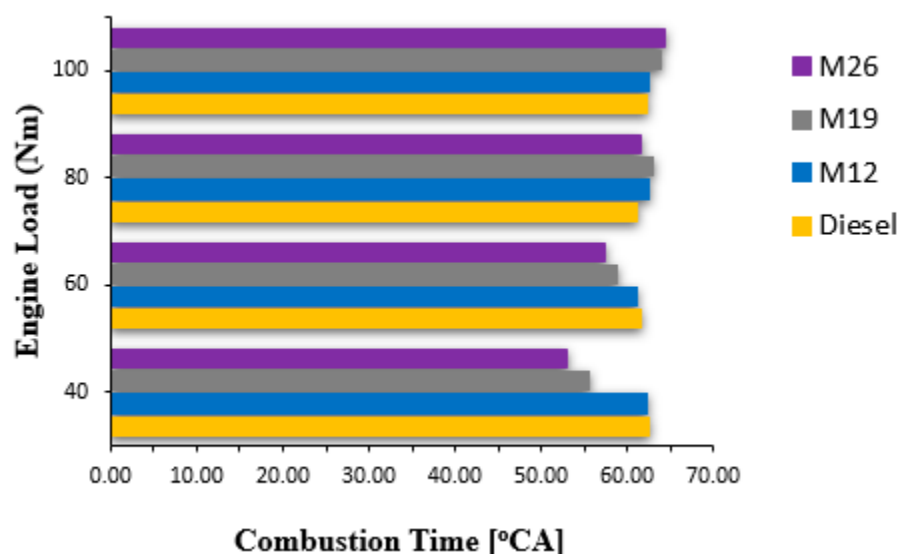


Figure 4. CDs in terms of °CA for different fuels at 40 Nm, 60 Nm, 80 Nm, and 100 Nm ELs.

The CD is found to be 61.17 °CA for diesel fuel, 62.58 °CA for M12 fuel, 62.93 °CA for M19 fuel, and 61.52 °CA for M26 fuel at an 80 Nm load. The CD obtained by using diesel fuel at an 80 Nm load increased by 2.31% with M12 fuel, 2.87% with M19 fuel, and 0.57% with the use of M26 fuel.

The CD at a 100 Nm load is found to be 62.23 °CA for diesel fuel, 62.58 °CA for M12 fuel, 63.98 °CA for M19 fuel, and 64.34 °CA for M26 fuel. The CD obtained by using diesel fuel at a 100 Nm load increased by 0.56% with M12 fuel, 2.81% with M19 fuel, and 3.39% with the use of M26 fuel.

In this study, the CD decreased with increasing methanol ratio at low loads (40 and 60 Nm), whereas it increased with the rising methanol ratio at high loads (80 and 100 Nm).

3.2. Engine Performance

3.2.1. Brake-Specific Fuel Consumption

Bsfc is defined as the unit amount of fuel consumed by the engine per unit of power produced. Figure 5 shows the amount of fuel consumed by the RCCI engine per unit of power for different fuel types. Bsfc is found to be 45.90 g/kWh for diesel fuel, 50.92 g/kWh for M12 fuel, 55.08 g/kWh for M19 fuel, and 58.42 g/kWh for M26 fuel at a 40 Nm load. The bsfc obtained by using diesel fuel at a 40 Nm load increased by 10.94% with M12 fuel, 20% with M19 fuel, and 27.28% with the use of M26 fuel.

Bsfc is found to be 55.83 g/kWh for diesel fuel, 62.42 g/kWh for M12 fuel, 68.40 g/kWh for M19 fuel, and 73.56 g/kWh for M26 fuel at a 60 Nm load. The bsfc obtained by using diesel fuel at a 60 Nm load increased by 11.80% with M12 fuel, 22.51% with M19 fuel, and 31.76% with the use of M26 fuel.

Bsfc is found to be 70.83 g/kWh for diesel fuel, 79.54 g/kWh for M12 fuel, 85.21 g/kWh for M19 fuel, and 86.21 g/kWh for M26 fuel at an 80 Nm load. The bsfc obtained by using diesel fuel at an 80 Nm load increased by 12.30% with M12 fuel, 20.30% with M19 fuel, and 21.71% with the use of M26 fuel.

Bsfc increases with increasing EL. The highest increase is 31.76% in M26 fuel at 60 Nm. Due to the high latent heat of evaporation, methanol reduces the in-cylinder temperature, thus requiring more fuel compared with diesel mode to provide the same power output. For this reason, it is thought that bsfc has increased [28]. The lower calorific value of the fuel increases the bsfc. In this study, more diesel fuel was injected to achieve the same power output.

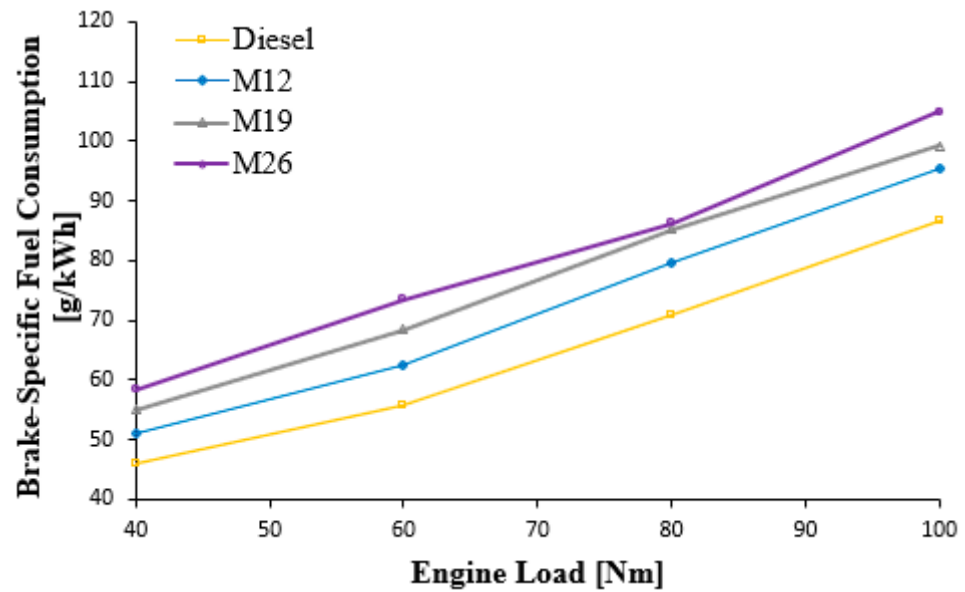


Figure 5. Bsfc in g/kWh for different fuels at 40 Nm, 60 Nm, 80 Nm, and 100 Nm ELs.

3.2.2. Brake-Specific Energy Consumption

Bsec is a parameter that depends on bsfc. The amount of fuel consumed by the engine per unit of power produced is called bsec. Examining bsec yields more meaningful results when comparing fuels with different calorific values. As seen in Figure 6, the energy consumed by the RCCI engine per unit power for different fuel types is shown. Bsec is found to be 1950.58 kJ/kWh for diesel fuel, 1962.07 kJ/kWh for M12 fuel, 2013.65 kJ/kWh for M19 fuel, and 1975.24 kJ/kWh for M26 fuel at a 40 Nm load. The bsec obtained by using diesel fuel at a 40 Nm load increased by 0.59% with M12 fuel, 3.23% with M19 fuel, and 1.26% with the use of M26 fuel.

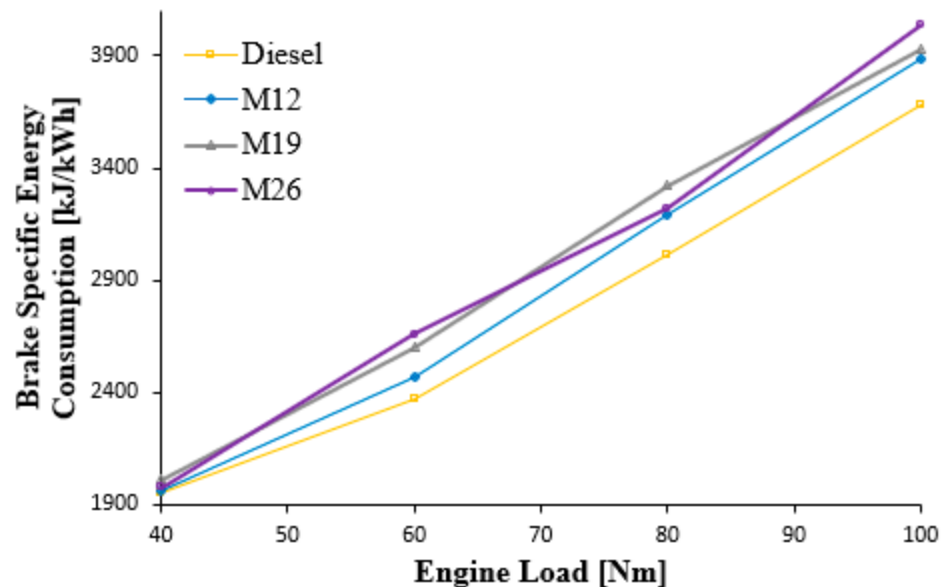


Figure 6. Bsec in kJ/kWh for different fuels at 40 Nm, 60 Nm, 80 Nm, and 100 Nm ELs.

Bsec is found to be 2372.90 kJ/kWh for diesel fuel, 2466.03 kJ/kWh for M12 fuel, 2598 kJ/kWh for M19 fuel, and 2658.13 kJ/kWh for M26 fuel at a 60 Nm load. The bsec obtained by using diesel fuel at a 60 Nm load increased by 3.92% with M12 fuel, 9.49% with M19 fuel, and 12.02% with the use of M26 fuel.

Bsec is found to be 3010.40 kJ/kWh for diesel fuel, 3193.73 kJ/kWh for M12 fuel, 3323.26 kJ/kWh for M19 fuel, and 3220.78 kJ/kWh for M26 fuel at an 80 Nm load. The bsec obtained by using diesel fuel at an 80 Nm load increased by 6.09% with M12 fuel, 10.39% with M19 fuel, and 6.99% with the use of M26 fuel.

Bsec is found to be 3683.35 kJ/kWh for diesel fuel, 3881.65 kJ/kWh for M12 fuel, 3927.51 kJ/kWh for M19 fuel, and 4034.69 kJ/kWh for M26 fuel at a 100 Nm load. The bsec obtained by using diesel fuel at a 100 Nm load increased by 5.38% with M12 fuel, 6.63% with M19 fuel, and 9.54% with the use of M26 fuel. As the methanol ratio and EL increased, bsec values also increased. The highest increase was 12.02% in M26 fuel at 60 Nm.

3.3. Emissions

Various exhaust emissions are released as a result of the combustion of petroleum-based hydrocarbon fuels or alternative fuels in ICEs. These emissions are released into the environment in different amounts and percentages. In today's internal combustion engines, harmful emissions must meet the low emission values specified in the norms through the use of after-treatment devices located after the exhaust valve. However, these applications cause both a decrease in engine performance and an increase in costs.

3.3.1. HC Emissions

Figure 7 shows HC emissions occurring at different loads. HC emissions at a 40 Nm load is 15.6 ppm with diesel fuel, 31.57 ppm with M12 fuel, 78 ppm with M19 fuel, and 113.17 ppm with M26 fuel. HC emissions obtained by using diesel fuel at a 40 Nm load increased by 102.37% with M12 fuel, 400% with M19 fuel, and 625.45% with the use of M26 fuel.

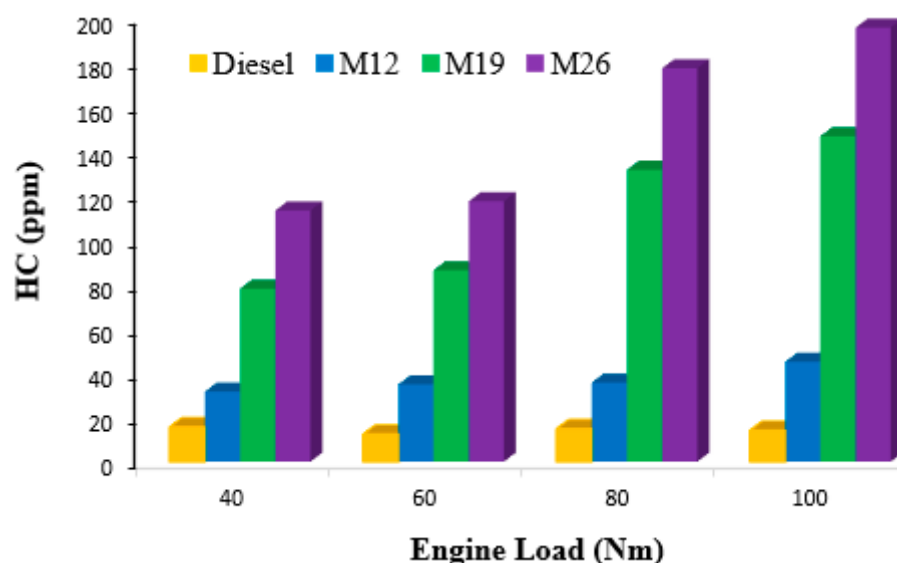


Figure 7. HC emissions for different fuels at 40 Nm, 60 Nm, 80 Nm, and 100 Nm ELs.

HC emissions at a 60 Nm load are 12.33 ppm with diesel fuel, 34.83 ppm with M12 fuel, 86.3 ppm with M19 fuel, and 117.35 ppm with M26 fuel. HC emissions obtained by using diesel fuel at 60 Nm load increased by 182.48% with M12 fuel, 599.92% with M19 fuel, and 751.74% with the use of M26 fuel.

HC emissions at an 80 Nm load are 14.80 ppm with diesel fuel, 35.67 ppm with M12 fuel, 131.57 ppm with M19 fuel, and 177.30 ppm with M26 fuel. HC emissions obtained by using diesel fuel at 80 Nm load increased by 141.01% with M12 fuel, 788.99% with M19 fuel, and 1097.97% with the use of M26 fuel.

HC emissions at a 100 Nm load are 14.07 ppm with diesel fuel, 45 ppm with M12 fuel, 146.7 ppm with M19 fuel, and 195.60 ppm with M26 fuel. HC emissions obtained by using

diesel fuel at 100 Nm load increased by 219.83% with M12 fuel, 942.64% with M19 fuel, and 1290.19% with the use of M26 fuel.

As the methanol ratio increases, hydrocarbon (HC) emissions also increase. Researchers have determined that the increase in high HC emissions during RCCI combustion mode is the main source of HC emissions, the thickness of the sudden cooling layer during combustion and the rich and premixed fuel and air mixture in this layer [29]. In another study, it was observed that HC emission increased in low-temperature combustion due to low combustion temperature and low oxygen concentration [30].

3.3.2. CO₂ Emissions

Although carbon dioxide does not have a direct effect on human and environmental health, half of the CO₂ resulting from combustion processes accumulates in the atmosphere, and this accumulation leads to an increase in the concentration of CO₂ in the atmosphere. Because CO₂ affects weather conditions, this increase affects the environment by creating a greenhouse effect in the atmosphere.

Figure 8 shows CO₂ emissions occurring at different ELs. At a 40 Nm load, CO₂ emissions are 4.2%vol with diesel fuel, 4.81%vol with M12 fuel, 4.49%vol with M19 fuel, and 4.23%vol with M26 fuel. CO₂ emissions obtained by using diesel fuel at a 40 Nm load increased by 14.52% with M12 fuel, 6.9% with M19 fuel, and 0.71% with M26 fuel.

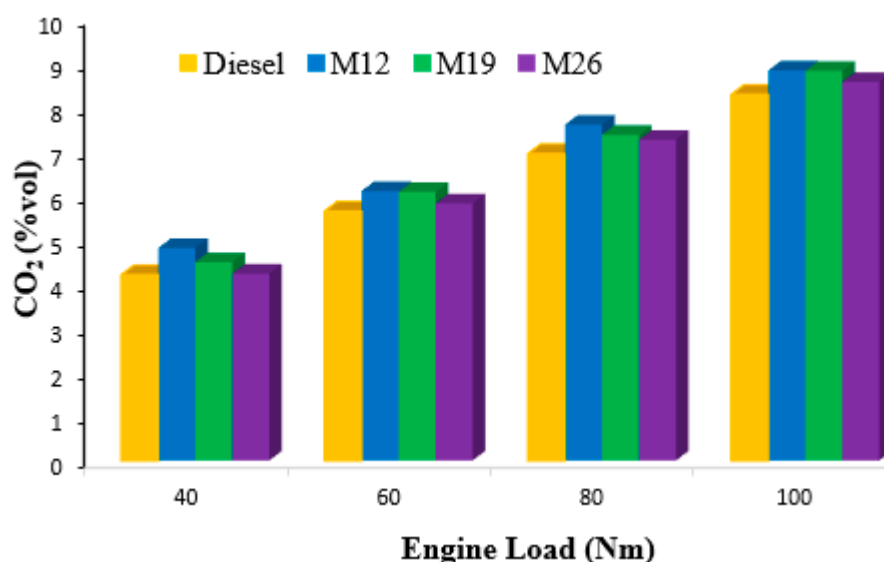


Figure 8. CO₂ emissions for different fuels at 40 Nm, 60 Nm, 80 Nm, and 100 Nm ELs.

At a 60 Nm load, CO₂ emissions are 5.64%vol with diesel fuel, 6.1%vol with M12 fuel, 6.08%vol with M19 fuel, and 5.82%vol with M26 fuel. CO₂ emissions obtained by using diesel fuel at a 60 Nm load increased by 8.16% with M12 fuel, 7.8% with M19 fuel, and 3.19% with M26 fuel.

At an 80 Nm load, CO₂ emissions are 6.94%vol with diesel fuel, 7.6%vol with M12 fuel, 7.37%vol with M19 fuel, and 7.26%vol with M26 fuel. CO₂ emissions obtained by using diesel fuel at an 80 Nm load increased by 9.51% with M12 fuel, 6.2% with M19 fuel, and 4.61% with the use of M26 fuel.

CO₂ emissions at a 100 Nm load are 8.28%vol with diesel fuel, 8.83%vol with M12 fuel, 8.82%vol with M19 fuel, and 8.57%vol with M26 fuel. CO₂ emissions obtained by using diesel fuel at 100 Nm load increased by 6.64% with M12 fuel, 6.52% with M19 fuel, and 3.5% with the use of M26 fuel.

In general, CO₂ increases as engine load increases. Because this is related to the amount of fuel burned in the cylinders, it increases because more fuel is burned. At the same ELs, it decreases as oxidation occurs as you move from M12 to M26.

According to research conducted in the literature, it has been determined that the CO₂ emission values obtained from diesel fuel–methanol blend fuels are lower than diesel fuel. The reason for this is that methanol contains fewer C atoms than diesel fuel. It is stated that as the C-atom ratio of blended fuels decreases, CO₂ emissions released as a result of combustion decrease [31].

3.3.3. O₂ Emissions

Figure 9 shows O₂ emissions occurring at different loads. At a 40 Nm load, O₂ emissions are 14.84%vol with diesel fuel, 14.04%vol with M12 fuel, 14.28%vol with M19 fuel, and 14.57%vol with M26 fuel. O₂ emissions obtained by using diesel fuel at a 40 Nm load decreased by 5.39% with M12 fuel, 3.77% with M19 fuel, and 1.82% with the use of M26 fuel.

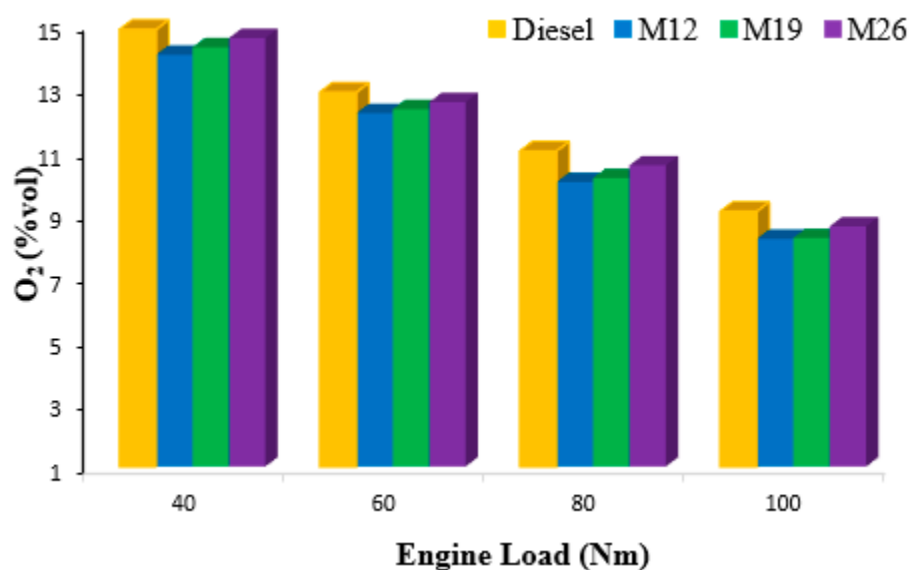


Figure 9. O₂ emissions for different fuels at 40 Nm, 60 Nm, 80 Nm, and 100 Nm ELs.

At a 60 Nm load, O₂ emissions are 12.85%vol with diesel fuel, 12.19%vol with M12 fuel, 12.32%vol with M19 fuel, and 12.54%vol with M26 fuel. O₂ emissions obtained by using diesel fuel at a 60 Nm load decreased by 5.14% with M12 fuel, 4.12% with M19 fuel, and 2.41% with the use of M26 fuel.

At an 80 Nm load, O₂ emissions are 10.99%vol with diesel fuel, 10.01%vol with M12 fuel, 10.14%vol with M19 fuel, and 10.54%vol with M26 fuel. O₂ emissions obtained by using diesel fuel at an 80 Nm load decreased by 8.92% with M12 fuel, 7.73% with M19 fuel, and 4.09% with M26 fuel.

O₂ emissions at a 100 Nm load are 9.08%vol with diesel fuel, 8.21%vol with M12 fuel, 8.24%vol with M19 fuel, and 8.61%vol with M26 fuel. O₂ emissions obtained by using diesel fuel at a 100 Nm load decreased by 9.58% with M12 fuel, 9.25% with M19 fuel, and 5.18% with the use of M26 fuel.

It is seen that O₂ emissions increase due to increased oxidation as we move from M12 to M26 fuel under the same EL conditions. O₂ emissions decrease with the increase in load.

3.3.4. NO_x Emissions

When combustion occurs at high temperatures, NO_x is formed as a result of the interaction of nitrogen in the air with oxygen. Two important factors affecting NO_x formation are combustion chamber temperature and air–fuel ratio. Additionally, chemical reaction rates play a decisive role in the formation of NO_x emissions. However, because chemical reaction rates depend on temperature, this is also among the factors affecting the formation of NO_x [32].

Figure 10 shows NO_x emissions occurring at different loads. At a 40 Nm load, NO_x emissions are 840.02 ppm with diesel fuel, 980.83 ppm with M12 fuel, 828.07 ppm with M19 fuel, and 718.43 ppm with M26 fuel. NO_x emissions obtained by using diesel fuel at a 40 Nm load increased by 16.76% with M12 fuel, decreased by 1.42% with M19 fuel, and 14.47% with the use of M26 fuel.

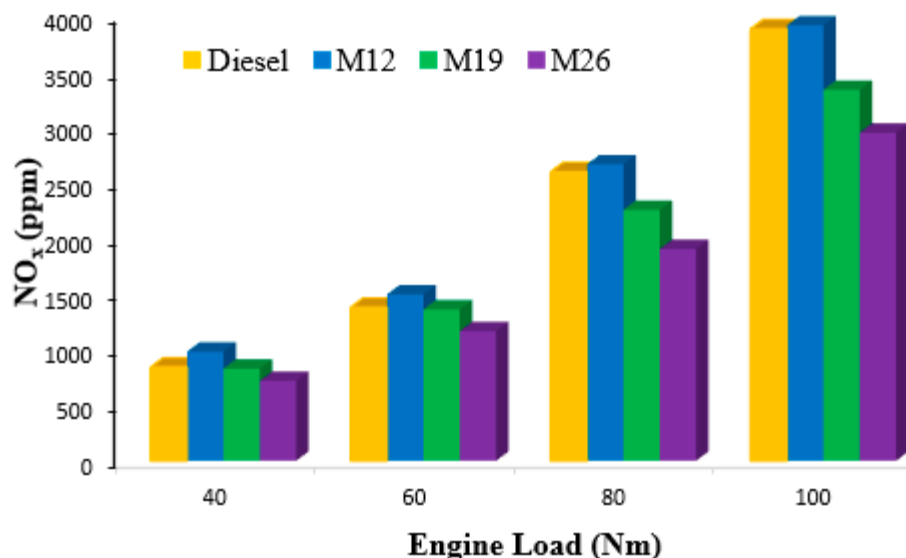


Figure 10. NO_x emissions for different fuels at 40 Nm, 60 Nm, 80 Nm, and 100 Nm ELs.

At a 60 Nm load, NO_x emissions are 1376.69 ppm with diesel fuel, 1494.47 ppm with M12 fuel, 1360.25 ppm with M19 fuel, and 1164.81 ppm with M26 fuel. NO_x emissions obtained by using diesel fuel at 60 Nm load increased by 8.56% with M12 fuel, decreased by 1.19% with M19 fuel, and 15.31% with the use of M26 fuel.

At an 80 Nm load, NO_x emissions are 2593.07 ppm with diesel fuel, 2662.77 ppm with M12 fuel, 2253.80 ppm with M19 fuel, and 1902.47 ppm with M26 fuel. NO_x emissions obtained by using diesel fuel at an 80 Nm load increased by 2.69% with M12 fuel, decreased by 13.08% with M19 fuel, and 26.63% with the use of M26 fuel.

NO_x emissions at a 100 Nm load are 3876.23 ppm with diesel fuel, 3911.27 ppm with M12 fuel, 3331.6 ppm with M19 fuel, and 2947.4 ppm with M26 fuel. NO_x emissions obtained by using diesel fuel at a 100 Nm load increased by 0.9% with M12 fuel and decreased by 14.05% with M19 fuel and 23.96% with the use of M26 fuel.

NO_x emissions increase with increasing EL. It decreases significantly as the methanol content and oxidation increases. The reason for the decrease in NO_x emissions as the methanol ratio increases is the high latent heat of evaporation of methanol. Methanol absorbs more heat from the environment during evaporation, causing the cylinder temperature to decrease. The amount of NO_x emissions increases with an increasing engine load. As more fuel is drawn into the cylinders, the instantaneous pressure ratio in the cylinder rises, leading to higher maximum pressure and combustion temperature. This effect results in an increase in NO_x emissions [33].

In a study by Benares et al., it was determined that a higher ID helped reduce NO_x emissions. It was observed that NO_x emissions increased at temperatures where maximum adiabatic flame temperatures were high [34]. This is consistent with the study in the literature, with the decrease in NO_x emissions at CAs where ID increases.

3.3.5. Smoke Emissions

In the diffusion-controlled combustion process that occurs in diesel engines, hydrogen reacts because hydrogen is generally more reactive towards oxygen than carbon, while carbons become smoke due to the effect of temperature, which takes time to complete the combustion and causes smoke formation, especially in cases where O₂ is insufficient.

Smoke is the solid carbon particles formed in this case. Generally, smoke formation is part of diesel combustion. Therefore, most of the initially formed carbon is burned again. As the EL increases, the amount of fuel sent to the combustion chamber also increases, which increases smoke formation because there is not enough O_2 in the cylinder [35].

Figure 11 shows the smoke emissions occurring at different ELs. At a 40 Nm load, smoke emissions are 0.1 m^{-1} with diesel fuel, 0.07 m^{-1} with M12 fuel, 0.06 m^{-1} with M19 fuel, and 0.05 m^{-1} with M26 fuel. Smoke emissions obtained by using diesel fuel at a 40 Nm load decreased by 30% with M12 fuel, 40% with M19 fuel, and 50% with M26 fuel.

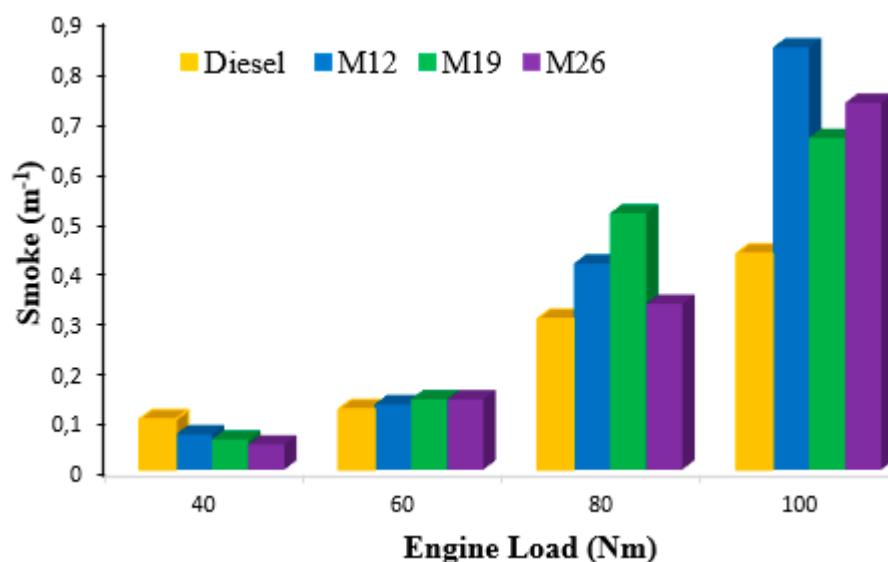


Figure 11. Smoke emissions for different fuels at 40 Nm, 60 Nm, 80 Nm, and 100 Nm ELs.

At a 60 Nm load, smoke emissions are 0.12 m^{-1} with diesel fuel, 0.13 m^{-1} with M12 fuel, 0.14 m^{-1} with M19 fuel, and 0.14 m^{-1} with M26 fuel. Smoke emissions obtained by using diesel fuel at a 60 Nm load increased by 8.33% with M12 fuel, 16.67% with M19 fuel, and 16.67% with M26 fuel.

At an 80 Nm load, smoke emissions are 0.3 m^{-1} with diesel fuel, 0.41 m^{-1} with M12 fuel, 0.51 m^{-1} with M19 fuel, and 0.33 m^{-1} with M26 fuel. Smoke emissions obtained by using diesel fuel at an 80 Nm load increased by 36.67% with M12 fuel, 70% with M19 fuel, and 10% with the use of M26 fuel.

At a 100 Nm load, smoke emissions are 0.43 m^{-1} with diesel fuel, 0.84 m^{-1} with M12 fuel, 0.66 m^{-1} with M19 fuel, and 0.73 m^{-1} with M26 fuel. Smoke emissions obtained by using diesel fuel at a 100 Nm load increased by 95.35% with M12 fuel, 53.49% with M19 fuel, and 69.77% with the use of M26 fuel.

As EL increased, smoke emissions also increased. According to a study, the increase in pilot fuel amount and energy rates as the engine load increases is one of the reasons affecting the increase in smoke emissions [36]. It is thought that smoke emission increases much faster at 80 and 100 Nm, and especially the increase in M12 and M19 fuels is due to the exposure of the diesel in the mixture to a higher temperature environment and also due to the decrease in oxygen availability [17].

4. Conclusions

RCCI engines are known as the LTC combustion concept using dual fuel. Using RCCI technology provides more controllable combustion over a wider operating range. This allows the engine to operate with higher efficiency while also reducing exhaust emissions.

Alcohol fuels are a type of fuel that can be an alternative to gasoline and diesel fuels. Methanol is an alcohol fuel with a high octane number. The fact that methanol has low NO_x and CO_2 emissions and can be obtained from renewable sources makes it attractive

for use as an alternative to motor fuels. The use of methanol in RCCI engines can provide significant advantages in terms of emission control.

The methanol energy fraction ratio has a significant impact on engine performance and emissions. This ratio determines the engine's operating characteristics and combustion efficiency. It is important to optimize energy fraction ratios and thus increase engine efficiency for the balanced use of methanol and diesel fuels in RCCI engines.

The unique contribution of this study is the detailed investigation of a part-load, four-cylinder, turbocharged diesel/methanol-fueled RCCI engine under different engine loads and methanol fraction ratios. The results obtained show how a number of important parameters affect the performance and emissions of this engine, such as ignition delay, combustion duration, bsfc, bsec, and exhaust emissions.

In this study, ID, CD, bsfc, bsec, and exhaust emissions of a four-cylinder, turbocharged diesel/methanol-fueled RCCI engine under different ELs, and different methanol fraction ratios were examined in detail. The important results of the experimental study are summarized below:

- In RCCI mode, as the methanol content increased, the ID also increased. The highest increase was 88.13% in M19 fuel at 40 Nm. It is seen that the ignition delay increases as the load increases. It is seen that ID decreases at high loads of 100 Nm for M19 and M26 fuels. This phenomenon can be attributed to the increase in in-cylinder temperatures resulting from the decrease in the energy fraction of methanol and the lower latent heat of vaporization of diesel compared to methanol.
- At low loads (40 and 60 Nm), CD decreases significantly, while at high loads (80 and 100 Nm) CD increases.
- Bsfc and bsec increased as the methanol ratio and engine load increased. As EL increases, Bsfc also increases. The highest increase in bsfc was in M26 fuel at 60 Nm with 31.76%, while the highest increase in bsec was in M26 fuel at 60 Nm with 12.02%. While the minimum bsfc in conventional diesel fuel was 45.9 g/kWh at 40 Nm, the highest bsfc in M26 fuel was 104.88 g/kWh at 100 Nm. Bsec reached its lowest value at 40 Nm at 1950.58 kJ/kWh on conventional diesel fuel and its highest value at 4034.69 kJ/kWh at 100 Nm on M26 fuel.
- As the methanol ratio increased, HC and O₂ emissions increased, while NO_x and CO₂ emissions decreased. While smoke emission decreased at low loads, it tended to increase at high ELs.

These findings can serve as a reference for future engine design and fuel development studies.

Author Contributions: Conceptualization, M.T. and I.T.Y.; Formal analysis, M.T. and I.T.Y.; Investigation, M.T.; Writing—original draft, M.T.; Writing—review & editing, M.T. and I.T.Y.; Supervision, C.S. and I.T.Y. All authors have read and agreed to the published version of the manuscript.

Funding: This research received no external funding.

Data Availability Statement: Data is contained within the article.

Conflicts of Interest: The authors declare no conflicts of interest.

Nomenclature

BMEP	Brake mean effective pressure
bsec	Brake-specific energy consumption
bsfc	Brake-specific fuel consumption
BTE	Brake thermal efficiency
CA	Crank angle
CO	Carbon monoxide
CO ₂	Carbon dioxide
COHR	Center of heat release

CD	Combustion duration
CHR	Cumulative heat release
CHR	Cumulative heat release
CP	Cylinder pressure
EGR	Exhaust gas recirculation
ES	Energy sharing
EL	Engine load
HR	Heat release
HC	Hydrocarbon
HCCI	Homogeneous charge compression ignition
ICE	Internal combustion engine
ID	Ignition delay
LHV	Lower heating values
LTC	Low-temperature combustion
NOx	Nitrogen oxide
O ₂	Oxygen
PCCI	Premixed charge compression ignition
RCCI	Reactivity-controlled compression ignition
ROHR	Rate of heat release
ROPR	Rate of pressure rise
SOI	Start of ignition
V	Volume

References

- Balki, M.K.; Temur, M.; Erdoğan, S.; Sarıkaya, M.; Sayin, C. The determination of the best operating parameters for a small SI engine fueled with methanol gasoline blends. *Sustain. Mater. Technol.* **2021**, *30*, e00340. [\[CrossRef\]](#)
- Balki, M.K.; Sayin, C.; Sarıkaya, M. Optimization of the operating parameters based on Taguchi method in an SI engine used pure gasoline, ethanol and methanol. *Fuel* **2016**, *180*, 630–637. [\[CrossRef\]](#)
- Balki, M.K.; Cavus, V.; Duran, İ.U.; Tuna, R.; Sayin, C. Experimental study and prediction of performance and emission in an SI engine using alternative fuel with artificial neural network. *Int. J. Automot. Eng. Technol.* **2018**, *7*, 58–64. [\[CrossRef\]](#)
- Verhelst, S.; Turner, J.W.G.; Sileghem, L.; Vancoillie, J. Methanol as a fuel for internal combustion engines. *Prog. Energy Combust. Sci.* **2019**, *70*, 43–88. [\[CrossRef\]](#)
- Pavlov, G.I.; Nakoryakov, P.V.; Sukhovaya, E.A. Development of silencer for lowpower internal combustion engines. *Procedia Eng.* **2017**, *206*, 1690–1695. [\[CrossRef\]](#)
- Valera, H.; Agarwal, A.K. Methanol as an Alternative Fuel for Diesel Engines. In *Methanol and the Alternate Fuel Economy*; Energy, Environment, and Sustainability; Springer: Singapore, 2017; pp. 9–33. [\[CrossRef\]](#)
- Moon, C.S. Estimations of the lethal and exposure doses for representative methanol symptoms in humans. *Moon Ann. Occup. Environ. Med.* **2017**, *29*, 44. [\[CrossRef\]](#)
- Sayin, C. Engine performance and exhaust gas emissions of methanol and ethanol–diesel Blends. *Fuel* **2010**, *89*, 3410–3415. [\[CrossRef\]](#)
- Yin, X.; Yue, G.; Liu, J.; Duan, H.; Duan, Q.; Kou, H.; Wang, Y.; Yang, B.; Zeng, K. Investigation into the operating range of a dual-direct injection engine fueled with methanol and diesel. *Energy* **2023**, *267*, 126625. [\[CrossRef\]](#)
- Feng, H.; Chen, X.; Sun, L.; Ma, R.; Zhang, X.; Zhu, L.; Yang, C. The effect of methanol/diesel fuel blends with co-solvent on diesel engine combustion based on experiment and exergy analysis. *Energy* **2023**, *282*, 128792. [\[CrossRef\]](#)
- Ning, L.; Duan, Q.; Chen, Z.; Kou, H.; Liu, B.; Yang, B.; Zeng, K. A comparative study on the combustion and emissions of a non-road common rail diesel engine fueled with primary alcohol fuels (methanol, ethanol, and n-butanol)/diesel dual fuel. *Fuel* **2020**, *266*, 117034. [\[CrossRef\]](#)
- Li, Y.; Ming, J.; Chan, Y.; Liu, Y.; Xie, M.; Wang, T.; Zhou, L. Parametric study and optimization of a RCCI (reactivity controlled compression ignition) engine fueled with methanol and diesel. *Energy* **2013**, *65*, 319–332. [\[CrossRef\]](#)
- Li, J.; Yang, W.; Zhou, D. Review on the management of RCCI engines. *Renew. Sustain. Energy Rev.* **2016**, *69*, 65–79. [\[CrossRef\]](#)
- Reitz, R.D.; Duraisamy, G. Review of high efficiency and clean reactivity controlled compression ignition (RCCI) combustion in internal combustion engines. *Prog. Energy Combust. Sci.* **2014**, *46*, 12–71. [\[CrossRef\]](#)
- Kokjohn, S.L.; Hanson, R.M.; Splitter, D.A.; Reitz, R.D. Fuel reactivity controlled compression ignition (RCCI): A pathway to controlled high-efficiency clean combustion. *Int. J. Engine Res.* **2011**, *12*, 209–226. [\[CrossRef\]](#)
- Kokjohn, S.L.; Reitz, R.D. Reactivity controlled compression ignition and conventional diesel combustion: A comparison of methods to meet light-duty NO_x and fuel economy targets. *Intern. J. Engine Res.* **2013**, *14*, 452–468. [\[CrossRef\]](#)
- Panda, K.; Ramesh, A. Parametric investigations to establish the potential of methanol based RCCI engine and comparison with the conventional dual fuel mode. *Fuel* **2021**, *308*, 122025. [\[CrossRef\]](#)

18. Agarwal, A.K.; Kumar, V.; Jena, A.; Kalwar, A. Fuel injection strategy optimization and experimental performance and emissions evaluation of diesel displacement by port fuel injected methanol in a retrofitted mid-size genset engine prototype. *Energy* **2022**, *248*, 123593. [[CrossRef](#)]
19. Duraisamy, G.; Rangasamy, M.; Govindan, N. A Govindan, Comparative study on methanol/diesel and methanol/PODE dual fuel RCCI combustion in an automotive diesel engine. *Renew. Energy* **2020**, *145*, 542–546. [[CrossRef](#)]
20. Hassan, Q.H.; Ridha, G.S.A.; Hafedh KA, H.; Alalwan, H.A. The impact of Methanol-Diesel compound on the performance of a Four-Stroke CI engine. *Mater. Today Proc.* **2021**, *42*, 1993–1999. [[CrossRef](#)]
21. Huang, F.; Li, L.; Zhou, M.; Wan, M.; Shen, L.; Lei, J. Effect of EGR on performance and emissions of a methanol–diesel reactivity controlled compression ignition (RCCI) engine. *J. Braz. Soc. Mech. Sci. Eng.* **2023**, *45*, 440. [[CrossRef](#)]
22. Liu, J.; Wu, P.; Ji, Q.; Sun, P.; Wang, P.; Meng, Z.; Ma, H. Experimental study on effects of pilot injection strategy on combustion and emission characteristics of diesel/methanol dual-fuel engine under low load. *Energy* **2022**, *242*, 123464. [[CrossRef](#)]
23. Singh, V.S.; Jain, S.; Karn, A.; Dwivedi, G.; Alam, T.; Kumar, A. Experimental Assessment of Variation in Open Area Ratio on Thermohydraulic Performance of Parallel Flow Solar Air Heater. *Arab. J. Sci. Eng.* **2023**, *48*, 11695–11711. [[CrossRef](#)]
24. Sandalci, T.; Karagoz, Y. Experimental investigation of the combustion characteristics, emissions and performance of hydrogen port fuel injection in a diesel engine. *Int. J. Hydrogen Energy* **2014**, *39*, 18480–18489. [[CrossRef](#)]
25. Zangana, L.M.K.; Yaseen, A.H.; Hassan, Q.H.; Mohammed, M.M.; Mohammed, M.F.; Alalwan, H.A. Investigated kerosene-diesel fuel performance in internal combustion engine. *Clean. Eng. Technol.* **2023**, *12*, 100591. [[CrossRef](#)]
26. Qi, D.H.; Geng, L.M.; Chen, H.; Bian, Y.Z.; Liu, J.; Ren, X.C. Combustion and performance evaluation of a diesel engine fueled with biodiesel produced from soybean crude oil. *Renew. Energy* **2009**, *34*, 2706–2713. [[CrossRef](#)]
27. Wang, S.; Viswanathan, K.; Esakkimuthu, S.; Azad, K. Experimental investigation of high alcohol low viscous renewable fuel in DI diesel engine. *Environ. Energy Manag. Res.* **2021**, *28*, 12026–12040. [[CrossRef](#)]
28. Wei, J.; He, C.; Lv, G.; Zhuang, Y.; Qian, Y.I.; Pan, S. The combustion, performance and emissions investigation of a dual fuel diesel engine using silicon dioxide nanoparticle additives to methanol. *Energy* **2021**, *230*, 120734. [[CrossRef](#)]
29. Gao, Z.; Curran, S.J.; Parks, J.E., II; Smith, D.E.; Wagner, R.M.; Daw, C.S.; Edwards, K.D.; Thomas, J.F. Drive cycle simulation of high efficiency combustions on fuel economy and exhaust properties in light-duty vehicles. *Appl. Energy* **2015**, *157*, 762–776. [[CrossRef](#)]
30. Imtenan, S.; Varman, M.; Masjuki, H.H.; Kalam, M.A.; Sajjad, H.; Fattah, M.I.A.I.M.R. Impact of low temperature combustion attaining strategies on diesel engine emissions for diesel and biodiesels. *Energy Convers. Manag.* **2014**, *80*, 329–356. [[CrossRef](#)]
31. Cheng, C.H.; Cheung, C.S.; Chana, T.L.; Lee, S.C.; Yao, C.D. Experimental investigation on the performance, gaseous and particulate emissions of a methanol fumigated diesel engine. *Sci. Total Environ.* **2008**, *389*, 115–124. [[CrossRef](#)]
32. Gonca, G.; Hocaoglu, M.F. Emission and in-cylinder combustion characteristics of a spark ignition engine operated on binary mixtures of gas and liquid fuels. *Int. J. Hydrog. Energy* **2023**, *52*, 1502–1518. [[CrossRef](#)]
33. Sayin, C.; Uslu, K.; Canakci, M. Influence of injection timing on the exhaust emissions of a dual-fuel CI engine. *Renew. Energy* **2008**, *3*, 1314–1323. [[CrossRef](#)]
34. Benajes, J.; Molina, S.; García, A.; Belarte, E.; Vanvolsem, M. An investigation on RCCI combustion in a heavy duty diesel engine using in cylinder blending of diesel and gasoline fuels. *Appl. Therm. Eng.* **2014**, *63*, 66–76. [[CrossRef](#)]
35. Pilusa, T.J.; Mollagee, M.M.; Muzenda, E. Reduction of vehicle exhaust emissions from diesel engines using the whale concept filter. *Aerosol Air Qual. Res.* **2012**, *12*, 994–1006. [[CrossRef](#)]
36. Papagiannakis, R.G.; Rakopoulos, C.D.; Hountalas, D.T.; Rakopoulos, D.C. Emission characteristics of high speed, dual fuel, compression ignition engine operating in a wide range of natural gas/diesel fuel proportions. *Fuel* **2010**, *89*, 1397–1406. [[CrossRef](#)]

Disclaimer/Publisher’s Note: The statements, opinions and data contained in all publications are solely those of the individual author(s) and contributor(s) and not of MDPI and/or the editor(s). MDPI and/or the editor(s) disclaim responsibility for any injury to people or property resulting from any ideas, methods, instructions or products referred to in the content.